Vertical Takeoff and Landing Wing Developed for Long Distance Flight and Stable Transit Flight

Daeil Jo and Yongjin (James) Kwon
Industrial Engineering, Ajou University, Suwon, South Korea
Email: j11129@naver.com, yk73@ajou.ac.kr

***Abstract*—With the rise of the public interests in the UAVs, the UAVs are becoming one of the important technological areas of the 4th industrial revolution era. For the UAVs, the fixed-wing type is advantageous, because it has a longer flight time than the multi-copter type, along with the faster speed. However, it requires a separate, lengthy, obstacle-free landing area, which can be difficult to find in the urban area. Additionally, it is not easy to safely land the fixed-wing type UAVs. Because of this, demand for the VTOL-type UAV is on the rise. The purpose of this study is to design and develop a VTOL capable of vertical landing and lift-off, as well as having appropriate thrust and lift during vertical, horizontal, and transition flights. We developed a formalized UAV development process, to provide a theoretical guideline to the development process. In order to determine the aerodynamic characteristics of the VTOL, we employed the 3D CAD & CAE methods, which can simulate the wind tunnel test for the optimal aerodynamic efficiency. Using the developed process, we determined the criteria for the internal modules that constitute the UAV, and we could assemble the airframe, considering the proper center of gravity. We conducted the SW setting for the flight adjustment and able to carry out the flight test accordingly. In the flight experiment, it was found that the developed process was adequate to provide a guideline to the successful design of the VTOL-type UAV.**

***Index Terms*—UAV, VTOL, fixed wing, drone, multi-copter, rotary wing, aircraft design, transition flight**

I. Introduction

As the era of the fourth industrial revolution is underway, the field of new technologies are continuously increasing. As a result, a variety of UAVs (unmanned aerial vehicles) has been developed and widely used. The fixed-wing type UAV is advantageous because it has a longer flight time than the multi-copter type UAV. But it has a limited space for the runway, especially in the urban area, for safe landing and takeoff [1]. The demand for VTOL (vertical takeoff and landing), which can take off and land vertically, is increasing because this type doesn't need a runway and can fly like an airplane.

The main purpose of this study is to develop a formalize design process of the VTOL and use that process to actually build and fly the VTOL UAV. Up to this date, any formalized VTOL development process is not available. By providing a theoretically supported, formalized development process, we can reduce the possible errors and be able to produce more stable VTOL UAV [2].

II. Study on VTOL Development

In this study, we have developed a UAV development process in order to help the engineers to better design and construct the UAV. The process is divided into 12 steps as shown in Fig. 1 and the details are further elaborated in 3 chapters, as shown in figures 2, 3 and 4 [3].

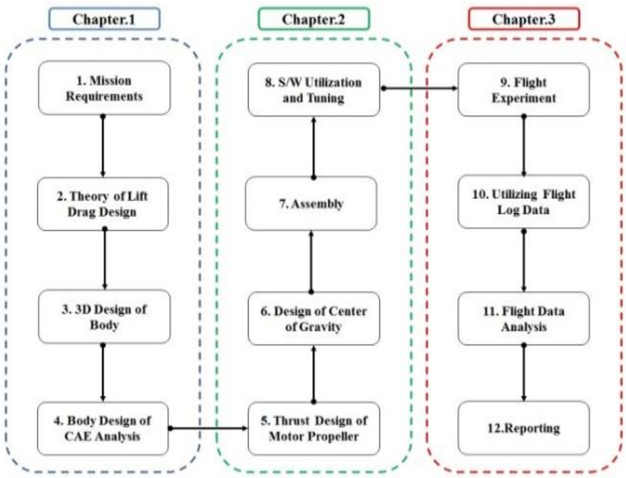

Figure 1. Development process of UAV

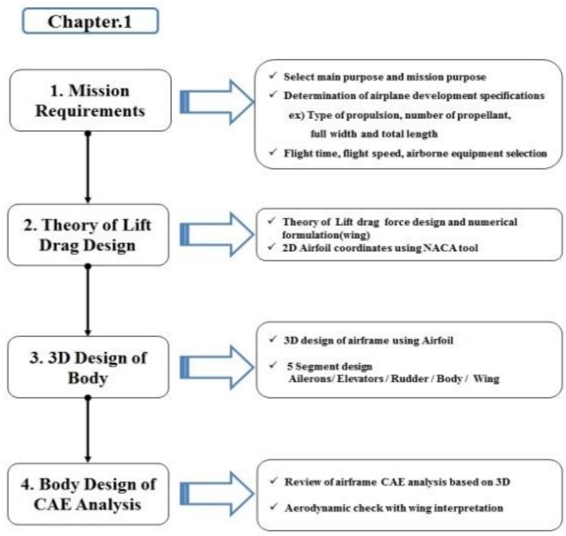

Figure 2. Development process of UAV Chapter 1

Manuscript received December 1, 2018; revised July 5, 2019.

doi: 10.18178/ijmerr.8.5.797-802

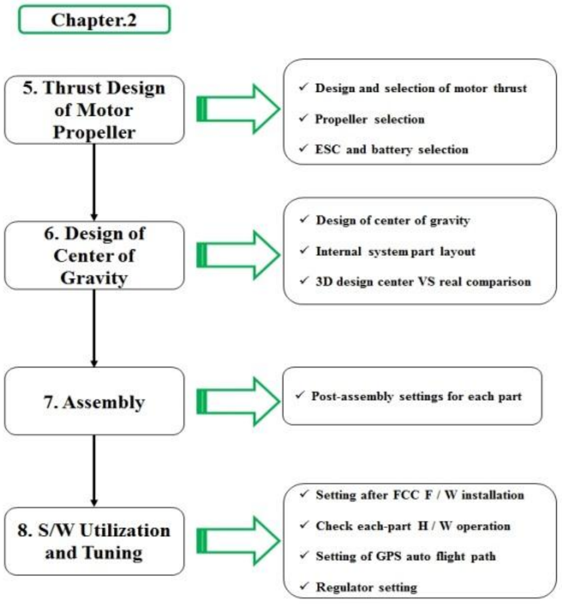

Figure 3. Development process of UAV Chapter 2

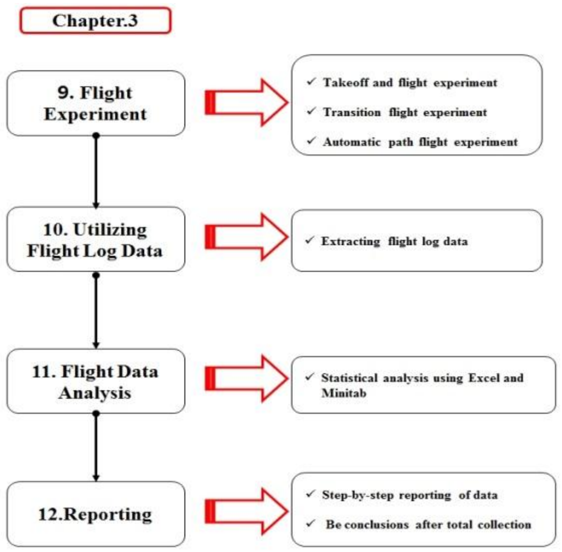

Figure 4. Development process of UAV Chapter 3

A. Establishment of Misiion Requirements

Figure 5 shows the mission profile of a VTOL UAV. Since it is a VTOL airframe, it is necessary to takeoff vertically and land vertically as well. When reaching the operating altitude, a transition flight is required to switch to a horizontal flight. All operations can be done by autopilot or the pilot can maneuver manually. Once the flight mission is over, the VTOL switches to the vertical landing mode, and gradually descend vertically and land on a designated spot. In this case, it is necessary to maintain the vertical posture and control the altitude through thrust control, just like the multi-copter type UAV. In either case, a smooth and stable transition flight is required. Due to this reason, the flight control of the VTOL type is more complicated than the wing-type or multi-copter type UAVs [4, 5].

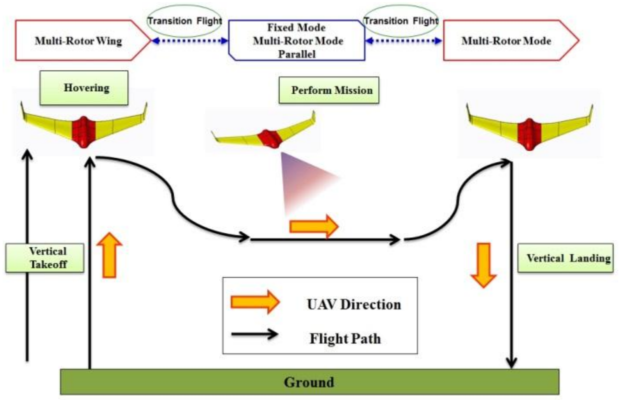

Figure 5. VTOL mission profile

B. Aerodynamic Design Using Airfoil

For the design of the wing, the lift and drag forces of the NACA-4412 airfoil were compared by numerical analysis with the reference to the information provided by the airfoiltools company. The parameters are set as follows. The wing-span was 2.1 m. The AOA was 3 °. The cold length was 0.2 m, and the altitude was 100 m, while the air density was 1.21 kg/m^3. The Reynolds number was 240,732 [6, 7].

TABLE I. Air Foil Speed for Lift (Unit: Kg)

	13m/s	14m/s	15m/s	16m/s	17m/s	18m/s	19m/s
NACA 4412	5.575	6.004	6.432	6.681	7.290	7.719	8.148

Table 1 shows the calculation results of the lift versus speed of each airfoil. The formula for lift and drag is shown in Equation (1).

$$Lift = \frac{1}{2}\mathrm{pv}^2\mathrm{SC}_L \quad (1)$$
$$Drag = \frac{1}{2}\mathrm{pv}^2\mathrm{SC}_D$$

The lift efficiency of NACA-4412 and the drag coefficient of NACA-4412 were obtained as follows: NACA-4412: C_L= 0.886, NACA-4412: C_D= 0.0118. The designed wing was calculated to produce as much lift as the weight of the entire airframe (6.43 kg), and could be lifted at an airframe speed of 15m/s [8].

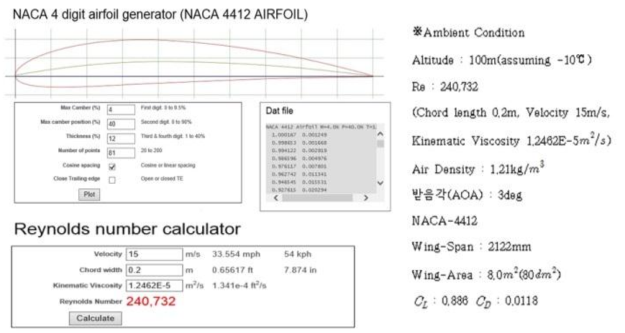

Figure 6. Wing design using the selected airfoil

C. Airframe 3D CAD Design for UAV

Figures 7 and 8 show the aircraft structure. The 3D CAD was used to design the NACA4412 wing- section, which studied the aerodynamic design with the length of

2240 x 711 x 160 mm. The airframe design is an essential part of the VTOL construction, because it is equipped with the FCC (flight control computer) and other various modules. In addition it should be designed as a streamlined and smoothly shaped airframe to reduce the air resistance. It was manufactured using Styrofoam material so that the weight of the airframe is minimized [9].

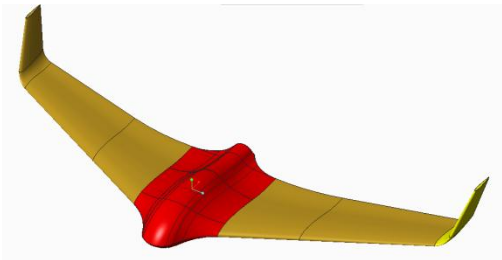

Figure 7. 3D design of airframe

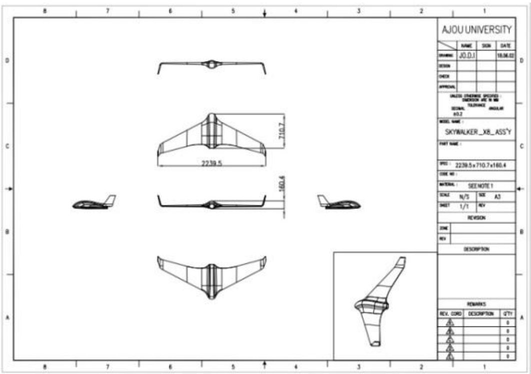

Figure 8. 2D layout of airframe

D. Airframe 3D CAE Analysis for UAV

In order to investigate aerodynamic design based on the theory after the airframe design, a simulation CAE was carried out to understand the airflow of the wing, which determines the flight performance. As shown in Fig. 9, the experimental conditions are boundary conditions when flying at 0 °C and 15m/s. The results of the analysis are summarized in terms of cross-section for a total of 300 seconds at intervals of 100 seconds. As shown in Fig. 10, it is found that the flow velocity and pressure are generated aerodynamically over time [10-15].

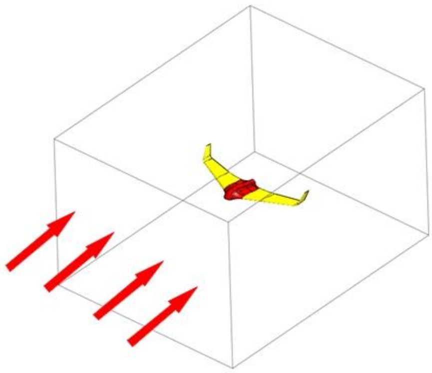

Figure 9. CAE experimental boundary condition

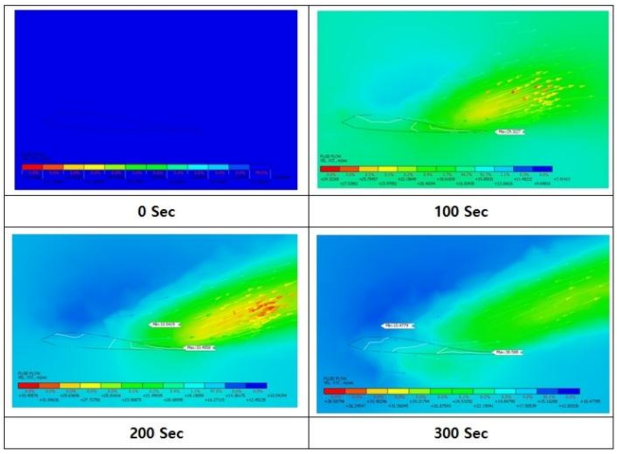

Figure 10. CAE simulation result

E. Design and Selection of Motor Thrust

The output is determined by the rotational speed of the motor and the propeller, and the thrust determination equation is shown in Equation (2). Also, the equation to determine the propeller for generating the thrust after determining the required thrust is shown in Equation (3).

$$Power = Prop\ Const * rpm^{Power\ factor} \quad (2)$$

$$T = \frac{\pi}{4} D^2 \rho v \Delta v \quad (3)$$

T : thrust[N]
D : propeller diameter[m]
v : velocity of air the propeller[m/s]
Δ *v : velocity of air the accelerated by propeller[m/s]*
ρ *: density of air[1.225 kg/*m^3 *]*

The standard for selecting the appropriate motor is shown in Fig.11.

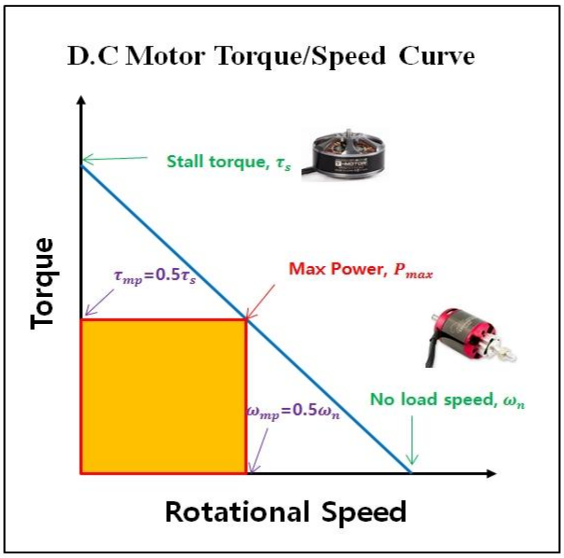

Figure 11. Motor torque / speed curve plot

In order to find the maximum output of the motor, one should check the number of revolutions at which the maximum output is generated. Referring to Fig. 11, it can be seen that the maximum torque is generated when the number of rotations is at 50% point. In a typical UAV flight, the matching of motor rotational directions and the torque of each motor is important. Hovering thrust should be at least equal to the weight of the airframe and the thrust is solely generated by the propellers. The hovering should be reached at half the maximum output of the motor and should occur at 50% of the battery voltage [16]. The DC motor is rated in Kv (Rpm/volts) and the number of revolutions at the maximum output is half of the motor's Kv/2 multiplied by the voltage of the battery. It is shown in the Equation (4).

$$\text{rpm}_{maxpower} = \frac{KV * 0.5 * Battery-Volts}{2} \qquad (4)$$

In order to select the propellers using this way, we calculate the weight of the VTOL UAV, by calculating the total weight as well as the weight of each component constituting the UAV. That is, the motor can be selected based on the weight derived from the airframe design stage.

F. Selection of Propellers

The specification of the propellers are distinguished as XXYY as shown in Fig12.

- XX: overall length of the propeller (unit: inch)
- YY: pitch of the propeller

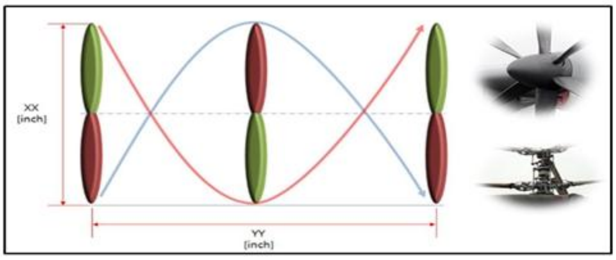

Figure 12. Propeller configuration

The greater the number of XX, the larger the magnitude, which means that a larger lift can be obtained. The larger the number of YY, the higher the lift can be achieved. The propeller should be large with a high pitch, but the weight of the propeller is increased as the battery consumption also increases accordingly. This leads to the decrease of the flight time. Therefore, it is necessary to select the proper propeller according to the size of the airframe and the specification of the motor. Based on the motor selected in this way, the propeller is selected using the Equation (5).

$$\boldsymbol{rpm_{ideal}} = \left(\frac{2}{\pi}\right)^{\frac{1}{2\omega}} \left(\frac{g^{\frac{3}{2}} m^{\frac{3}{2}}}{\alpha D \sqrt{\rho}}\right)^{1/\omega} \qquad (5)$$

ω = *Power Factor from Aircraft*
α = *Power Coefficient from Aircraft*
D = Diameter[m]
ρ = *Air Density [1.225kg/m^3]*
m =Mass [kg]
g= Gravity [9.8m/s^2]

G. Selection of Battery

The battery in this study was selected as 6 Cell, 22.2 V, 10,000 mAh type, considering flight time and thrust. Here, the 'mAh' indicates the capacity of the battery. For example, an indication of 100,000 mAh means that you can use 1 hour when you draw 10,000 mA. The 'V' indicates the voltage. One must use a battery with the proper voltage to stabilize the current to drive motors. The 'Wh' shows how much power the battery has. This value can be calculated by multiplying the capacity mAh with the voltage V. The 'C' indicates the discharge rate. For instance, the meaning of '3S 10000mAh 15C' means that it can output 15 times and it can discharge up to 10000 x 15 = 150A.

The battery is directly related to the flight time, and Equation (6) represents the flight time according to the capacity and the consumption current of the battery.

$$\textit{Flight time} = \textit{Battery capacity/amps} \qquad (6)$$

$$\textit{Flight time} = 10000mAh * \frac{60min}{(hour)} * \frac{1}{(40A)} * \frac{A}{(10000mA)} = 24 \text{ min}$$

H. Center of Gravity

In 3D design, the center of gravity is shown as 440mm from the end to the center as shown in Fig.13.

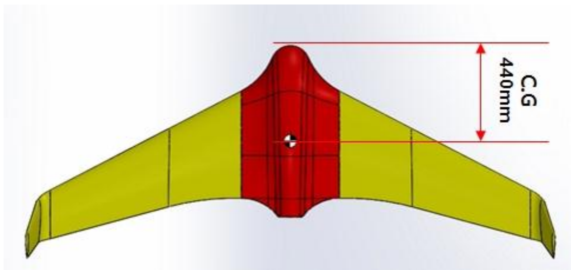

Figure 13. Center of gravity

However, when the actual modules are placed, the center of gravity is different from the design value. As shown in Fig.14, it is necessary to review the consideration of the center of gravity appropriate to the actual product after arranging the modules in the airframe [17-19]. The assembly process is shown in figures 15 and 16.

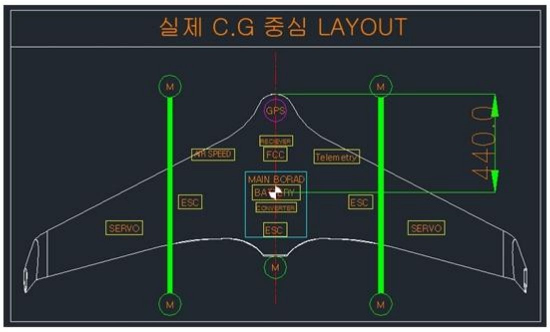

Figure 14. Product module relocation LAYOUT

I. Assembly & SW setup

As shown in Fig.15, the designed UAV was manufactured by using Styrofoam and 3D printer, and assembled by referring to the layout of each module to establish the center of gravity. In order to make the VTOL 'H' type, a motor and a propeller were added by attaching a carbon fiber column to the airframe as shown in Fig.18. In order to provide a vertical height from the ground, a supporting frame is constructed by 3D printer and attached, as shown in Fig.17. The completed VTOL UAV is shown in Fig. 18.

The GCS (ground control station) SW is required to set up and operate the finished UAV. FCC is selected as a PixHawk type. In order to operate the UAV properly, we downloaded the Mission Planner GCS SW from the Ardupilot site to set up the UAV parameters [19-21].

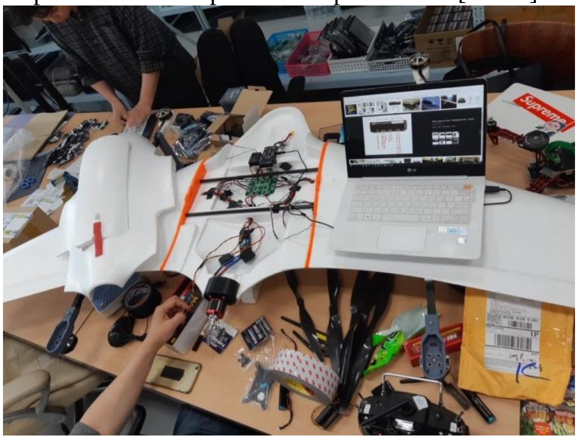

Figure 15. Assembling internal component modules

Figure 16. Airframe attached with carbon fiber columns

Figure 17. Floor support made with 3D printer

Figure 18. Completed UAV appearance

J. Flight Experiment

After completion of the airframe construction, setting up of the center of gravity, as well as the flight parameters, we analyzed the VTOL flight characteristics by conducting numerous test flights. The test results revealed that the VTOL was effectively performing in all flights including the takeoff, transition, horizontal, and landing. Fig. 19 shows the results of the flight experiment.

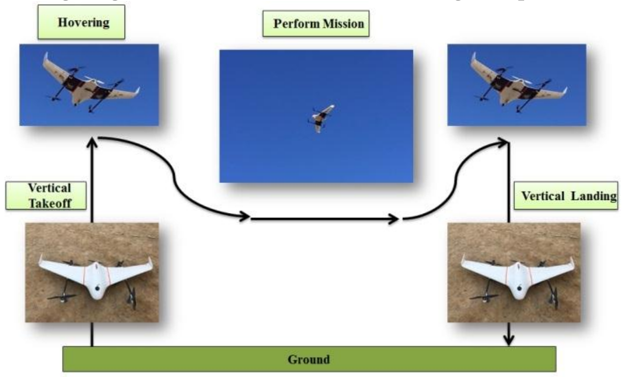

Figure 19. Flight step-by-step experiment

K. Flight Data Analysis

It is possible to analyze the flight data by referring to the log data that can be extracted from the FCC after the flight test was over. For instance, as shown in Fig.20, a stable hovering is verified. If the throttle cruise value is between the range of 0 and 1,000, a stable hovering is performed. In this test flight, it seems that the proper hovering was done between 80 and 300 [22-25].

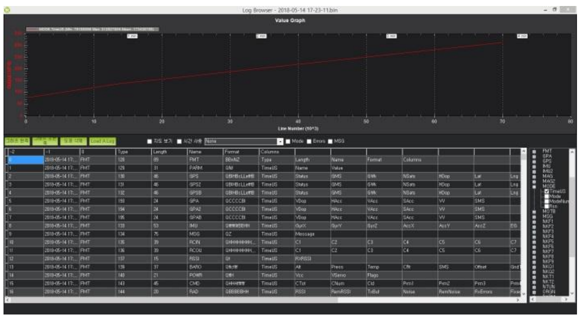

Figure 20. Flight hovering data

III. Conclusion

To analyze the effectiveness of the proposed UAV development process, the specifications of the VTOL UAVs are compared as shown in Table 2. The one on the left is the previously constructed VTOL UAV by us without using the proposed development process. It did not consider the important aeronautical design factors properly, as opposed to in this study. Due to this reason, the previously developed VTOL has a trouble with the center of gravity during the transition flight, as well as the aerodynamic efficiencies during the horizontal flight. As a result, one can apply the formalized UAV development process that has been proposed in this study, in order to save the potential errors.

TABLE II. Specification Comparison of Study

Spec	Existing Study	This Study
Figure		
Length	1,200 mm	1,000 mm
Wing Span	1,950 mm	2,200 mm
Empty Weight	3.9 Kg	4.6 Kg
Velocity	15~18 m/s	15~24 m/s
Flight Time	20 min	40 min
Lift	3 Kg	7 Kg
Vertical Thrust	12 Kg	15 Kg
Center of gravity	Not Considered	Considered
Aerodynamics	Not Considered	Considered
Systematic	Not Applied	Applied

Acknowledgment

Following are the result of a study on the "Leaders in Industry-university Cooperation +" Project, supported by the Ministry of Education and National Research Foundation of Korea.

Reference

[1] J. D. I. and Y. J. Kwon, “Analysis of VTOL UAV propellant technology,” *Journal of Computer and Communications*, vol. 5, pp. 76-82, May 2017.

[2] D. I. JO and Y. J. Kwon, “Development of rescue material transport UAV,” *World Journal of Engineering and Technology*, vol. 5, pp. 720-729, Oct 2017.

[3] M. A .Erbil, S. D. Priro, M. Karamanoglu, S. Odedra, C. Barlow, D. Lewis, “Reconfigurable unmanned aerial vehicles,” *The international Conference on Manufacturing and Engineering System*, pp. 392-396, 2009.

[4] K. B. Kim, “Design and verification of multi-rotor based unmanned aerial vehicle system,” Ph.D. Dissertation, Dept. of Mechanical Eng., Konkuk Univ., South Korea, 2013.

[5] D. H. Shim, H. J .Kim, Sastry, “Control system design for rotorcraft-based unmanned aerial vehicles using time-domain system identification,” *IEEE International Conference on Control Application*, pp. 808-813, 2000.

[6] O. S. An, “Development of Tiltrotor flight airframe and development of high speed VTOL,” *Aerospace Industry Technology Trend*, vol. 5, no.1, pp. 75-92, 2007.

[7] Y. N. Kang, “Development trend of control technology for unmanned aircraft,” *Aerospace Industry Technology Trend*, vol. 4, no. 2, pp. 55-67, 2006.

[8] E. S. Choi, “Performance analysis of propeller using ground stopping thrust test and feather element theory,” *Korean Society for Aeronautical & Space Sciences Spring Conference*, 2006.

[9] C. J. Lee, *Aircraft Structural Design Practice: Good Land-Company*, USA, 2017.

[10] M. Kevadiya, “CFD analysis of pressure coefficient for NACA 4412,” *International Journal of Engineering Trends and Technology (IJETT)*, vol. 4, no. 5, pp. 2041-2043, May 2013.

[11] P. B. Makwana, “Numerical simulation of flow over airfoil and different techniques to reduce flow separation along with basic CFD model,” *International Journal of Engineering Research & Engineering (IJETT)*, vol. 3, no. 4, pp. 419-429, Aug. 2014.

[12] S. J. Yun, Aerodynamics: Saintian Company, 2010.

[13] Aircraft Design Education Research Group, Aircraft concept design: Kyeongmun Company, 2012.

[14] MIDAS IT, Structural Analysis, 2018.

[15] MIDAS IT, Flow analysis, 2018.

[16] W. E. Green and P. Y. Oh, “Autonomous hovering of a fixed-wing micro air vehicle,” *IEEE International Conference of Automation (ICRA)*, 2006.

[17] O. S. An, “Development and design of vertical takeoff and landing aircraft,” *Korean Physics Society*, vol. 15, no.5, 2006.

[18] D. Kubo, S. Suzuki, “Tail-sitter vertical takeoff and landing unmanned aerial vehicle: Transitional flight analysis,” *Journal of Aircraft*, vol. 45, no. 1, pp. 292-297, 2008.

[19] S. Yu, J Heo, S. Jeong, and Y. J. Kwon, “Technical analysis of VTOL UAV,” *Journal of Computer and Communications*, vol. 4, pp. 92-97, May 2016.

[20] W. E. Green, P. Y. Oh, “Optic-flow-based collision avoidance - applications using a hybrid MAV,” *IEEE Robotics and Automation Magazine*, vol. 15, no. 1, pp. 96-103, 2008.

[21] E. N. Johnson, A. Wu, J. C. Neidhoefer, S. K. Kannan, M. A. Turbe, “Flight-test results of autonomous airplane transitions between steady-level and hovering flight,” *Journal of Guidance Control and Dynamics*, vol. 31, no. 2, pp. 358-370, 2008.

[22] K. Kita, A. Konno, M. Uchiyama, “Hovering control of a tail-sitter VTOL aerial robot,” *Journal of Robotics and Mechatronics*, vol. 21, no. 2, pp. 277-283, 2009.

[23] U. Ozdemir, “Design of a commercial hybrid VTOL UAV system,” *Journal of Intelligent & Robotic Systems*, vol. 74, no. 1-2, pp. 371-393, April 2014.

[24] B. Herisse, F. X. Russotto, T. Hamel, and R. Mahony, “Hovering flight and vertical landing control of a VTOL unmanned aerial vehicle using optical flow,” in *Proc. of IEEE/RSJ International Conference on Intelligent Robots and Systems (IROS)*, pp. 801-806, 2008.

[25] S. Park, “Accurate modeling and robust hovering control for a quad-rotor VTOL aircraft,” in *Proc. 2nd International Symposium on UAVs*, pp. 9-26. June 2009.

Daeil Jo has many years of engineering experience in industrial engineering and mechanical engineering.
He has experience concerning R&D and manufacturing in Field. He carried out research applied to industrial engineering concepts of unmanned aerial systems. He has great interest in CAD & CAE and UAV. He received his master's degree from Ajou University. .

Yongjin (James) Kwon has many years of engineering experience in industrial and academic settings. He has extensive experience & practical knowledge in current design, manufacturing and quality control. His work has been cited a number of times in high profile journals. He is currently a professor in the Department of Industrial Engineering at Ajou University. Prior to joining Ajou, he was on the faculty of Drexel University, Philadelphia, USA.